

6-2012

Paramecium bursaria Chlorella Virus 1 Proteome Reveals Novel Architectural and Regulatory Features of a Giant Virus

David Dunigan

University of Nebraska - Lincoln, ddunigan2@unl.edu

Ronald Cerny

University of Nebraska-Lincoln, rcerny1@unl.edu

Andrew T. Bauman

Ocean Biologics, Seattle, WA

Jared C. Roach

Institute of Systems Biology, Seattle, WA

Leslie C. Lane

University of Nebraska - Lincoln, llane1@unl.edu

See next page for additional authors

Follow this and additional works at: <http://digitalcommons.unl.edu/virologypub>



Part of the [Virology Commons](#)

Dunigan, David; Cerny, Ronald; Bauman, Andrew T.; Roach, Jared C.; Lane, Leslie C.; Agarkova, Irina V.; Wulser, Kurt William; Yanai-Balser, Giane M.; Gurnon, James R.; Vitek, Jason C.; Kronschnabel, Bernard J.; Jeannard, Adrien; Blanc, Guillaume; Upton, Chris; Duncan, Gary; McClung, O. William; Ma, Fangrui; and Van Etten, James L., "Paramecium bursaria Chlorella Virus 1 Proteome Reveals Novel Architectural and Regulatory Features of a Giant Virus" (2012). *Virology Papers*. 226.
<http://digitalcommons.unl.edu/virologypub/226>

This Article is brought to you for free and open access by the Virology, Nebraska Center for at DigitalCommons@University of Nebraska - Lincoln. It has been accepted for inclusion in Virology Papers by an authorized administrator of DigitalCommons@University of Nebraska - Lincoln.

Authors

David Dunigan, Ronald Cerny, Andrew T. Bauman, Jared C. Roach, Leslie C. Lane, Irina V. Agarkova, Kurt William Wulser, Giane M. Yanai-Balser, James R. Gurnon, Jason C. Vitek, Bernard J. Kronschnabel, Adrien Jeannard, Guillaume Blanc, Chris Upton, Gary Duncan, O. William McClung, Fangrui Ma, and James L. Van Etten

1 Title: *Paramecium bursaria* Chlorella Virus 1 Proteome Reveals Novel Architectural and
2 Regulatory Features of a Giant Virus

3 David D. Dunigan[#] (1, 2), Ronald L. Cerny (3), Andrew T. Bauman (4), Jared C. Roach (5),
4 Leslie C. Lane (1), Irina V. Agarkova (1, 2), Kurt Wulser (3), Giane M. Yanai-Balser (1), James
5 R. Gurnon (1), Jason C. Vitek (1), Bernard J. Kronschnabel (1), Adrien Jeannard (6), Guillaume
6 Blanc (6), Chris Upton (7), Garry A. Duncan (8), O. William McClung (8), Fangrui Ma (2),
7 James L. Van Etten[#] (1, 2)

8 ¹Department of Plant Pathology, University of Nebraska-Lincoln, Lincoln, NE 68583-0900,
9 USA;

10 ²Nebraska Center for Virology, University of Nebraska-Lincoln, Lincoln, NE 68583-0900,
11 USA;

12 ³Department of Chemistry, University of Nebraska-Lincoln, Lincoln, NE 68588-0304, USA;

13 ⁴Ocean Biologics, Seattle, WA 98133, USA

14 ⁵Institute of Systems Biology, Seattle, WA 98103, USA;

15 ⁶Structural and Genomic Information Laboratory, UMR7256 CNRS, Aix-Marseille University,
16 Marseille, FR-13385, France

17 ⁷Department of Biochemistry and Microbiology, University of Victoria, Victoria, British
18 Columbia, Canada;

19 ⁸Department of Biology, Nebraska Wesleyan University, Lincoln, NE 68504-2794, USA

20 Running title: PBCV-1 virion proteome

21 Key words: Chlorella, Phycodnaviridae, large dsDNA virus, protein mass-spectrometry

22 Abstract: 174 words

23 Text: 7,017 words

24 [#]Corresponding authors: David Dunigan, email: ddunigan2@unl.edu and James L. Van Etten,
25 email: jvanetten1@unl.edu

26 **ABSTRACT**

27 The 331 kilobase pairs chlorovirus PBCV-1 genome was re-sequenced and
28 annotated to correct errors in the original 15 year old sequence; forty codons was
29 considered the minimum protein size of an open reading frame. PBCV-1 encodes 416
30 predicted protein encoding sequences and 11 tRNAs. A proteome analysis was also
31 conducted on highly purified PBCV-1 virions using two mass-spectrometry based
32 protocols. The mass spectrometry-derived data were compared to PBCV-1 and its host
33 *Chlorella variabilis* NC64A predicted proteomes. Combined, these analyses revealed
34 148 unique virus-encoded proteins associated with the virion (about 35% of the coding
35 capacity of the virus) and one host protein. Some of these proteins appear to be
36 structural/architectural, whereas others have enzymatic, chromatin modification and
37 signal transduction functions. Most (106) of these proteins have no known function or
38 homologs in the existing gene databases except as orthologs with other chloroviruses,
39 phycodnaviruses and nuclear-cytoplasmic large DNA viruses. The genes encoding these
40 proteins are dispersed throughout the virus genome and most are transcribed late or early-
41 late in the infection cycle, which is consistent with virion morphogenesis.

INTRODUCTION

42
43 Complex cellular and viral processes are modular and accomplished by the
44 concerted action of functional modules. One of the important functional modules of a
45 virus is the virion particle, which ranges in complexity from a single type protein and
46 small nucleic acid (e.g., tomato bushy stunt virus) to having dozens of types of proteins
47 and lipids, along with a large nucleic acid genome (e. g., poxviruses). Regardless,
48 whether “simple” or complex in composition, all virions carry the legacy of their
49 progenitors through encapsidation, release and stabilization. Virions facilitate
50 propagation of progeny through a series of tightly regulated biochemical steps, called the
51 immediate-early phase of infection, which includes attachment, penetration, uncoating of
52 the viral genome, intracellular trafficking of the viral genome to its replication center, and
53 augmentation of cellular functions to “accept” the exotic nucleic acid/replicon. The
54 architectural elements of virions tend to be prominent, but studies on the supergroup
55 nucleocytoplasmic large DNA viruses (NCLDV) (7, 37, 43) indicate that in addition to
56 structural components, these virions perform multiple enzymatic and regulatory functions
57 that are partitioned among several proteins. The purpose of this study was to determine
58 the virion proteome of *Paramecium bursaria* chlorella virus 1 (PBCV-1), a member of
59 the NCLDV (11, 54).

60 PBCV-1 is the type member of the genus *Chlorovirus* (family *Phycodnaviridae*)
61 that infects certain chlorella-like green algae from fresh water sources; these viruses are
62 found throughout the world (54, 56). The chlorovirus host algae are normally symbionts
63 of aquatic protists, and in this state are resistant to virus infection. Nevertheless, virus
64 titers from natural sources have been measured as high as 10^5 plaque forming units (pfu)

65 per ml; however, titers fluctuate with the season (58, 61). Very little is known about the
66 role chloroviruses play in freshwater ecology (41), but susceptible hosts lyse within 6-16
67 hours in the laboratory and burst sizes typically exceed 10^2 pfu per cell (54, 56). Thus,
68 chloroviruses have the potential to alter microbial communities both quantitatively and
69 qualitatively, as well as act as a driving force for microbial evolution (11). Fortunately,
70 some of the host algae can be grown in the laboratory independent of their co-symbiotic
71 protists.

72 The 331 kilobase pair (kbp) PBCV-1 dsDNA genome was sequenced and
73 annotated about 15 years ago (26) and reported to have 689 open reading frames (ORF)
74 of at least 65 codons. Of these 689 ORFs, 377 were predicted to encode proteins (CDS);
75 PBCV-1 also encoded 11 tRNAs (reviewed in 21, 55, 57). The size of PBCV-1 extends
76 beyond its coding capacity; the virion is a $T = 169d$ quasi-icosahedral particle with a
77 diameter of 190 nm across the 5-fold axis (63, 64) and has an estimated molecular mass
78 of greater than 1×10^9 Da (53). The virion is ~64% protein consisting of at least 40
79 polypeptides, as seen on one dimensional SDS-PAGE (42). The particle contains 5-10%
80 lipid, which is associated with a bi-layered membrane underneath an outer glycoprotein
81 shell (5, 42, 64).

82 The capsid structure consists of the major capsid protein (MCP, Vp54), which is
83 glycosylated at 6 sites (31) and is myristylated at least at one site (36). Vp54 complexes
84 with itself, and perhaps other proteins, to form homotrimeric capsomers that are
85 responsible for the planar features of the capsid. Initially it was assumed that, except for
86 the 12 vertices, Vp54 was the only protein contributing to the external capsid and 5040
87 copies of Vp54 were predicted per virion (64). However, recent studies indicate that the

88 PBCV-1 virion is more complex than previously thought. i) PBCV-1 contains a unique
89 vertex with a 560-Å-long spike structure, which protrudes 340 Å from the surface of the
90 virus. The part of the spike structure that is outside of the capsid has an external diameter
91 of 35 Å at the tip, expanding to 70 Å at the base. The spike structure widens to 160 Å
92 inside the capsid and forms a closed cavity inside a large pocket between the capsid and
93 membrane enclosing the virus DNA (5, 66). The related chlorovirus CVK1 has a virion-
94 associated protein Vp130 (homolog of PBCV-1 A140/145R) that binds to algal cell walls
95 and is located at a unique vertex (34, 35), suggesting this protein is associated with the
96 spike structure. ii) Regularly spaced appendages occurring on the surface of the virion
97 are present at approximately 1 per trisymmetron (66). These appendages probably assist
98 in attaching the virion to its host cell (56). iii) The volume of the capsomers at the
99 common vertices and those surrounding the spike structure at the unique vertex differ
100 significantly, suggesting they consist of different proteins (5, 66). iv) At least one vertex
101 region may have a retractable appendage, such that when probed with a scanning atomic
102 force stylet the structure retracts, but then resets much like a plunger with a spring (23).
103 It is not known if this plunger is at the unique spike structure vertex or one of the other 11
104 vertices. v) Six minor capsid proteins of varying stoichiometries support the particle
105 architecture and appear to interact with the internal membrane in both the tri- and
106 pentasymmetron structures, as observed with an 8.5 Å resolution map of the virion (66).
107 Of these, a “long protein” (~32 kDa) with similarity to the PRD1 bacteriophage long
108 glue proteins forms an hexagonal network over the internal surface of the trisymmetrons,
109 and a “membrane protein” dimer (~28 kDa) is located at the edge of the trisymmetrons
110 and is connected to the internal membrane (1, 8). vi) PBCV-1 DNA binding proteins

111 were evaluated with proteomic methods from isolated viral DNA of virions (59). Six
112 proteins were identified that have high isoelectric points that are well suited for binding
113 and neutralization of DNA. Thus, PBCV-1 structure has both symmetric and asymmetric
114 elements, adding to the complexity of the virus morphology.

115 vii) In addition to these structural features, PBCV-1 contains several functions
116 that initiate infection. PBCV-1 attaches specifically to its host *Chlorella variabilis*
117 NC64A. Thus, we predict one or more surface proteins of the virus mediate attachment;
118 it is probably the spike structure (66). Immediately upon PBCV-1 attachment, the cell
119 wall is degraded at the site of attachment. viii) Virions contain cell wall degrading
120 activity (28, 62). ix) Within the first minutes of infection the cell membrane depolarizes
121 (12, 32), leaving the cell with significantly altered secondary transporter functions (2).
122 This activity is hypothesized to be partially due to a PBCV-1-encoded K⁺ channel, Kcv
123 (A250R) (27); however, no direct evidence supports the presence of Kcv in the virion. x)
124 In the first five min of infection host DNA begins to degrade and this is likely due to the
125 two virus-encoded DNA restriction endonucleases [R.CviAI (A579L), R.CviAII
126 (A252R)] packaged in PBCV-1 virions (3). Host chromatin degradation begins before
127 viral transcripts appear. PBCV-1 DNA is resistant to the restriction enzymes because it is
128 methylated. xi) The next major intracellular event is the synthesis of early viral
129 transcripts, observed 5-10 min p.i. (67; Blanc et al., unpublished data), which apparently
130 occurs by pirating the cellular transcriptional machinery, because the virus does not
131 encode a recognizable RNA polymerase gene and no polymerase activity was detected in
132 virion-derived extracts (Jon Rohozinski and James Van Etten, unpublished results).

133 The purpose of the current study is to evaluate the total viral complement of

134 proteins associated with the PBCV-1 virion using proteomic technologies and to re-
135 examine the structural/architectural features of this virus, as well as the initial events of
136 infection in the context of the protein complement. This evaluation led to the re-
137 sequencing of the PBCV-1 genome after preliminary proteomic analyses suggested there
138 were errors in the PBCV-1 genome sequence (26). This report presents the newly revised
139 PBCV-1 genome and annotations, and proteomic analyzes of the infectious particles.

140 MATERIALS AND METHODS

141 **Virus, cells, and culture conditions.** Procedures for growing virus PBCV-1 in
142 the alga *C. variabilis* have been described (3, 52, 53).

143 **Virus purification scheme.** The virus was purified essentially as described (52)
144 with the following modifications. Prior to sucrose density gradient separation, the virus-
145 cell lysate (2 liters) was clarified by incubating with 1% (v/v) NP-40 detergent at room
146 temperature for 1 - 2 h with constant agitation followed by centrifugation in a Beckman
147 Type19 rotor at 53,000 \times g, 50 min, 4°C. The pellet fraction was solubilized in virus
148 storage buffer (VSB) (50 mM Tris-HCl, pH 7.8) and layered onto a 10 - 40% (w/v) linear
149 sucrose density gradient made up in VSB, centrifuged in a Beckman SW28 rotor for 20
150 min at 72,000 \times g at 4°C. The virus band was identified by light scattering, removed from
151 the gradient and concentrated by centrifugation. Resuspended virus was incubated with
152 50 μ g/ml proteinase K in VSB for 4 h at 25°C to disassociate and degrade contaminating
153 proteins (this treatment has no effect on virus infectivity). The proteinase K treated virus
154 was layered onto a 20 - 40% linear iodixanol (OptiPrep™, Axis-Shield, Oslo, Norway)
155 gradient in VSB and centrifuged at 72,000 \times g in a Beckman SW28 rotor for 4 h at 25°C
156 for isopycnic separation. The gradient produced a single major light-scattering band at

157 ~32% iodixanol corresponding to a density of 1.171 g/ml. The virus band was removed
158 by side-puncture of the centrifugation tube, diluted approximately 10 fold with VSB, then
159 concentrated by centrifugation in a Beckman Ti50.2 rotor at 80,000 ×g for 3 h at 4°C.
160 The pellet fraction was re-suspended in VSB, then filter sterilized with a 0.45 µm cutoff
161 membrane, and stored at 4°C. The virus was quantified by UV/visible scanning
162 spectroscopy using an extinction coefficient of $A_{260/0.1\%} = 10.7$ (52) and plaque assayed to
163 determine the number of infectious particles. These preparations typically yielded
164 several milliliters of stock virus at 1 - 10 × 10¹¹ pfu/ml. The infectious to total particle
165 ratio is normally 0.25 - 0.5 for such preparations (53).

166 These preparations were used both for re-sequencing the PBCV-1 genome and the
167 determination of the proteome; the proteome was determined by two independent
168 methods using mass spectrometry of trypsin digested proteins.

169 **Re-sequencing and annotation of the PBCV-1 genome.** Preliminary proteomic
170 analyzes using the existing PBCV-1 gene annotations (NCBI Refseq: NC_000852)
171 revealed possible errors in the genome sequence, which prompted us to re-sequence the
172 PBCV-1 genome. PBCV-1 DNA was purified from virions treated with DNase I,
173 sequenced using Roche 454 Life Sciences GS FLX Titanium chemistry, and assembled
174 as described in the Supplemental Information section (SI). PBCV-1 contigs were
175 identified and annotated as described in the SI.

176 **Proteomics method 1. SDS-PAGE/Trypsin/HPLC/Ion Spray/MS-MS.**

177 **Particle disruption and protein extraction.** The PBCV-1 virion proteome was
178 evaluated with two independent methodologies, see Figure 1. In the first method virion
179 proteins were solubilized essentially as described (25) with reduction of the proteins by

180 adjusting 50 μg of virions in 50 μl . An equal volume of cracking buffer [50 mM Tris pH
181 8.5, 5 mM of the reducing agent dithiothreitol (freshly reduced with tributylphosphine; in
182 some experiments beta-mercaptoethanol was substituted for dithiothreitol), 1% SDS,
183 0.1% crystal violet and 1% Ficoll 400] was added. The sample was heated to 100°C for 3
184 min. The reduced proteins were subsequently alkylated by adjusting the solution to 12.5
185 mM iodoacetamide with a 0.25 M stock, then heating to 100°C for 1 min. These samples
186 were immediately subjected to SDS-PAGE. Alternatively, the proteins were alkylated
187 without previous reduction by the same procedure.

188 Alternatively, phenolic extractions were used to isolate virion proteins. Reduced
189 and alkylated proteins were adjusted to 40% sucrose to increase the density of the
190 solution. These preparations were then extracted with an equal volume of water-
191 saturated phenol or water-saturated phenol with toluene added to increase the
192 hydrophobicity of the phenol. The protein-containing phenolic phase was removed, and
193 protein was precipitated with 10 volumes of methanol then dissolved and heated in
194 cracking buffer.

195 **One-dimensional SDS-PAGE.** Proteins were separated on thirty-two cm linear
196 gradient (4-20%) polyacrylamide gels with 0.1% SDS and 375 mM Tris, pH 8.7 tank
197 buffer of 25 mM Tris/190 mM glycine. The samples were electrophoresed at room
198 temperature till the crystal violet tracking dye reached the bottom of the gel.

199 The gel was fixed and stained with Sypro-Ruby according to the manufacturer's
200 recommendation (Life Technologies Corporation). The stained gel was imaged using a
201 blue box transilluminator. Once imaged, the gel was cut into 32 one cm size pieces being
202 careful to clean the scalpel between samples. These gel pieces were then processed for

203 trypsin-digestion and mass spectrometry analyses.

204 **MS-based microsequencing.** Excised gel pieces were digested for peptide
205 sequencing using a slightly modified version of a method described by (40). Briefly, the
206 samples were washed with 100 mM ammonium bicarbonate, reduced with 10 mM DTT,
207 alkylated with 55 mM iodoacetamide, washed twice with 100 mM ammonium
208 bicarbonate, and digested *in situ* with 10 ng/ μ l trypsin. Peptides were extracted with two
209 60 μ l aliquots of 1:1 acetonitrile:water containing 1% formic acid. The extracts were
210 reduced in volume to approximately 25 μ l using a vacuum centrifugation.

211 Ten μ l of the extract solution was injected onto a trapping column (300 μ m x 1
212 mm) in line with a 75 μ m x 15 cm C18 reversed phase LC column (LC- Packings).
213 Peptides were eluted from the column using a water + 0.1% formic acid (A)/95%
214 acetonitrile:5% water + 0.1% formic acid (B) gradient with a flow rate of 270 μ l/min.
215 The gradient was developed with the following time profile: 0 min 5% B, 5 min 5% B, 35
216 min 35% B, 40 min 45% B, 42 min 60% B, 45 min 90% B, 48 min 90% B, 50 min 5% B.

217 The eluting peptides were analyzed using a Q-TOF Ultima tandem mass
218 spectrometer (Micromass/Waters, Milford, MA) with electrospray ionization. Analyses
219 were performed using data-dependent acquisition (DDA) with the following parameters:
220 1 sec survey scan (380-1900 Da) followed by up to three 2.4 sec MS/MS acquisitions
221 (60-1900 Da). The instrument was operated at a mass resolution of 8,000. The
222 instrument was calibrated using fragment ion masses of doubly protonated Glu-
223 fibrinopeptide.

224 **Mass ion analyses.** The MS/MS data were processed using Masslynx software
225 (Micromass) to produce peak lists for database searching. MASCOT (Matrix Science,

226 Boston, MA) was used as the search engine. Data were searched against the NCBI non-
227 redundant database. The following search parameters were used: mass accuracy 0.1 Da,
228 enzyme specificity trypsin, fixed modification CAM, variable modification oxidized
229 methionine. Protein identifications were based on random probability scores with a
230 minimum value of 25. Although this number varied from experiment to experiment,
231 typically it was 25 or less for $p < 0.05$ confidence.

232 **Relative abundances.** Approximate, relative quantitation of the proteins was
233 determined using the exponentially modified protein abundance index (emPAI) (18).
234 This method uses the number of observed peptides compared to the number of observable
235 peptides giving a ratio that is directly proportional to relative abundance of the protein in
236 the mixture when adjusted exponentially ($\text{emPAI} = 10^{\text{PAI}} - 1$; where PAI = number of
237 observed peptides per protein/number of observable peptides per protein).

238 **Proteomics method 2. PPS/Trypsin/HPLC/MS-MS**

239 **Protein extraction and trypsin digest.** One hundred μg of PBCV-1 was mixed
240 1:1 with 100 mM ammonium bicarbonate buffer pH 8.3 containing 0.2% PPS (Protein
241 Discovery Labs, San Diego, CA) [final concentration 50 mM ammonium bicarbonate,
242 0.1% PPS], boiled for 5 min, cooled to room temperature, reduced and alkylated with 5
243 mM dithiothreitol and 15 mM iodoacetamide, then digested with sequencing grade
244 trypsin at a 1:50 trypsin:protein ratio, for 4 h at 37°C, with shaking. The digested
245 samples were acidified with HCl (200 mM), incubated at 37°C, and centrifuged at 4°C, to
246 remove PPS prior to LC-MS application.

247 **LC Methods.** Buffer solutions were made with LC-MS grade water, acetonitrile,
248 and formic acid and consisted of 5% acetonitrile/0.1% formic acid in water (Buffer A)

249 and 100% acetonitrile/0.1% formic acid (Buffer B). Two or 4 μg total protein from each
250 sample was loaded onto a reverse phase (RP) trap (5 μm , 200 \AA , Magic; Michrom
251 Bioresources, Auburn, CA) with 100% buffer A and washed for 10 min prior to
252 separation on a microcapillary column. The microcapillary column was constructed by
253 slurry packing 18 cm of C18 material (2.7 μm , 100 \AA , HALO, Michrom Bioresources)
254 into a 75 μm ID fused silica capillary, which was previously pulled to a tip diameter of 5
255 μm using a Sutter Instruments laser puller (Sutter Manufacturing, Novato, CA).
256 Separations were performed on an Eksigent 1D+ nano-LC (Eksigent, Dublin, CA) LCQ-
257 Deca XP Plus: 0-30% B over 240 min, 30-70% B over 10 min at 300 $\mu\text{l}/\text{min}$; LTQ-Velos:
258 0-30% B over 80 min, 35-70% B over 10 minutes at 300 $\mu\text{l}/\text{min}$.

259 **Mass Spectrometry Methods.** Data-dependent tandem mass spectrometry
260 (MS/MS) analysis was performed using an LTQ-Velos or LCQ Deca XP Plus mass
261 spectrometer (ThermoFisher, San Jose, CA). Full MS spectra were acquired in centroid
262 mode, with a mass range of 400–2000 Da. To prevent repetitive analysis, dynamic
263 exclusion was enabled with a LTQ-Velos: repeat count of 1, a repeat duration of 30 sec,
264 an exclusion list size of 500, and an exclusion-duration of 90 sec. Tandem mass spectra
265 were collected using a normalized collision energy of 35% and an isolation window of 3
266 Da.

267 For the LTQ one full scan was followed by 6 MS-MS scans of the 6 most intense
268 precursor ions not on the dynamic exclusion list. LCQ-Deca XP Plus: repeat count of 1,
269 a repeat duration of 30 sec, an exclusion list size of 100, and an exclusion-duration of 20
270 sec. Tandem mass spectra were collected using a normalized collision energy of 35%
271 and an isolation window of 4 Da.

272 For the LCQ one full scan was followed by 3 MS-MS scans of the 3 most intense
273 precursor ions not on the dynamic exclusion list.

274 **Mass ion analyses.** Processing and searching of MS/MS spectra and analyzing
275 peptide and protein identification data were performed using SPIRE (Systematic Protein
276 Investigative Research Environment, www.proteinspire.org) system with default
277 parameters. Searches were conducted using the X!Tandem search engine (9) within a
278 2.5-Da mass error, a variable modification for methionine oxidation (16@M), and a fixed
279 modification for iodoacetamide (57@C) along with the default search parameters. The
280 sequence file for the searches of the modules contained PBCV-1 appended to a decoy
281 database of *Ostreococcus tauri*. In addition, a randomly reshuffled version of each
282 database was appended for error estimation. The search results were processed with the
283 LIPS (logistic identification of peptide sequences) model (16) to generate peptide spectra
284 scores. Peptide identification probabilities and FDRs were calculated based on the
285 reshuffled matches using an isotonic regression model (17). A 90% certainty was used as
286 the basis for spectra identifications. A recently introduced approach was used to estimate
287 the protein identification FDR from individual peptide identification probabilities (17).

288 RESULTS AND DISCUSSION

289 **Re-sequenced and re-annotated PBCV-1 genome.** The original sequence and
290 annotation of PBCV-1 was completed over 15 years ago using primitive procedures when
291 compared to current technology. During the past 15 years we have corrected the
292 sequence of individual genes as mistakes were detected. Those mistakes and preliminary
293 results from the current proteomic analyses that indicated sequencing errors, prompted us

294 to re-sequence PBCV-1. The revised PBCV-1 genome contains 330,805 nucleotide pairs
295 compared to 330,743 nucleotide pairs from the earlier sequencing effort. The two
296 genome versions differed by 458 indel positions (mostly single nucleotide indels) and
297 188 substitutions. This genome sequence and annotation are deposited at the National
298 Center for Biotechnology Information (NCBI) as reference sequence NC_000852.5; the
299 genome annotation is listed in SI Table S1. The re-sequenced genome submitted to
300 NCBI includes the 2,222 base pair terminal inverted repeat ends, but not the incompletely
301 base-paired covalently closed hairpin 35-nucleotide loops at each end of the genome.
302 Thus, the genome is a linear double-stranded DNA of 330,805 base pairs with two 35-
303 nucleotide partially paired terminal loops. Sequencing reads were obtained through the
304 hairpin loops (data not shown). When compared to the published results from Zhang et al.
305 (1994), the terminal repeats and hairpin loops are identical. Nucleotide 1 refers to the first
306 paired nucleotide following the hairpin loop.

307 One significant change in the new annotation is that ORFs of 40 codons or more
308 were classified as potential CDSs; the previous annotation used 65 codons as the
309 minimum size. This resulted in 802 ORFs, of which 416 ORFs were classified as
310 “major” CDSs (designated with an upper case “A”) based on the following supporting
311 evidence: these ORFs did not have larger overlapping ORFs and/or were expressed
312 transcriptionally (65) and/or the protein was identified in the proteomic analyses. The
313 major ORFs cover 92.8% of the genome sequence and have an average protein product
314 size of 249 amino acids. In addition, 11 tRNA genes were identified as reported
315 previously. The remaining 386 ORFs were labeled “minor” ORFs (designated with a
316 lower case “a”) and most of them are probably not CDSs. They encode putative proteins

317 with an average size of 86 amino acids. The gene annotations, along with functional
318 assignments, are listed in SI Table S1.

319
320 To avoid confusion in the literature, we kept the same gene numbering system as
321 used previously, i.e., a gene labeled as *a250r* is still labeled *a250r*. When two adjacent
322 ORFs were found to be a single ORF, e.g., A189R and A192R, we named it A189/192R.
323 Finally, where smaller ORFs were identified that were not considered previously, we
324 labeled them with a lower case letter, e.g., A254aR. These new gene annotations were
325 used for the proteomic analyses of the virion proteins.

326 **PBCV-1 virion proteome.** Highly purified virions were used for the proteome
327 analyses, including a "protease treatment" step where the particles were incubated with
328 proteinase K to degrade proteins non-specifically associated with the particle surface.
329 Proteinase K treatment does not affect PBCV-1 infectivity (3). Using a combination of
330 sample treatment, separation and mass spectrometry methods, 148 virus-encoded proteins
331 were detected in the PBCV-1 virion (Fig. 2B). For abundant proteins, any method was
332 sufficient to detect mass ions allowing identification with high confidence. However,
333 some of the low abundance and small proteins were only identified by one of the two
334 methods, primarily due to differential separation where the protein of interest was
335 separated from an abundant, and consequently masking, protein. The dynamic range of
336 these analyses was $\sim 10^4$ with the MCP present at approximately 10^3 copies per virion
337 relative to a hypothetical protein present at one copy per virion. Thus, the sample
338 treatment and separation method selected were important elements in the proteome
339 determination. The proteins were identified by two independent methods, 62% of the
340 proteins were detected by both methods. Twenty six percent were uniquely identified

341 with the SDS-PAGE method (Method 1) and 11% were uniquely identified with the PPS
342 solubilization method (Method 2). It is important to note some proteins are not readily
343 detected using mass spectrometric methods, e. g., small proteins associated with
344 membranes (39). Thus, the proteome reported here may increase with additional data in
345 the future. However, the results presented are the compilation of many experiments
346 using varying conditions for protein extraction and isolation giving us high confidence in
347 the compiled list of proteins including several proteins with predicted transmembrane
348 domains, as well as many small proteins; i. e., less than 10 kDa (Table 1).

349 **Method 1. SDS-PAGE/Trypsin/HPLC/Ion Spray/MS-MS.** Method 1
350 identified 137 virus-encoded proteins in the virion. Virion proteins were either: i)
351 extracted directly into gel sample buffer, ii) first extracted into a phenolic phase to
352 remove nucleic acids, or iii) extracted into a hypo-polarized phenolic phase supplemented
353 with toluene to further extract highly polar proteins such as glycosylated proteins. The
354 extracted proteins were either alkylated with iodoacetamide and then reduced, or left
355 alkylated. While these methods helped extract certain proteins, others were excluded and
356 no additional proteins were detected beyond the standard method of extracting into the
357 gel sample buffer.

358 Protein separation using one-dimensional gel electrophoresis resolved ~30 distinct
359 SYPRO-Ruby stained bands. The dynamic range of observed polypeptides is large. For
360 example, the MCP migrates at approximately 54 kDa and is the most abundant protein in
361 the virion, migrating near the mid-point of the gel (Fig. 2A, gel position 13). The MCP
362 has a nominal mass of 48 kDa and is post-translationally modified with sugars at 6
363 positions (31) and with at least one myristyl group (36), as well as having the amino

364 terminal methionine removed (13). This very abundant protein contrasts to proteins
365 detected in regions of the gel where little or no staining was observed, e. g., gel positions
366 #1, 8, 9, 31, 32 in Fig. 2A. Although very little staining was observed in these regions,
367 several proteins were detected by the mass spectrometry analyses. Indeed, proteins were
368 detected in all regions of the gel.

369 Qualitative changes in protein mobility were observed with different sample
370 treatments (SI Fig. S1). Samples that were alkylated with iodoacetamide, gave nearly the
371 same number of bands as those that were reduced with dithiothreitol (or beta-
372 mercaptoethanol) and alkylated. However, the mobility of a few proteins was altered by
373 this differential treatment, as visualized by SYPRO-Ruby staining. For example, a
374 protein band(s) migrating at gel position #5 in the alkylated sample is absent in the
375 sample that was both reduced and alkylated. Conversely, proteins observed at gel
376 positions 7 and 8 for the reduced and alkylated sample are not visible in samples only
377 alkylated. Several other differentials occurred between these two treatments;
378 nevertheless, the protein profiles determined for these treatments were similar for the
379 prominent proteins. The use of multiple treatment and separation methods was most
380 useful for low abundant polypeptides as indicated by MASCOT score.

381 **Method 2. Trypsin/HPLC/MS-MS.** The trypsin/HPLC/MS-MS method
382 identified 126 virus-encoded proteins, 16 of which were unique to this method. All
383 tryptic or semi-tryptic peptide matches were analyzed using the SPIRE analysis suite (14-
384 17) against PBCV-1 and *C. variabilis* genome databases. Restricting the matches to
385 tryptic only peptides did not decrease the false positive rate, so full semi-tryptic searching
386 was employed. The false positive rate was estimated from searches of a decoy database

387 of the *Ostreococcus tauri* proteome. The false positive rate was computed to be 0.42%,
388 so one of the 126 proteins identified in this group of experiments might be a false
389 positive. All the proteins identified had a confidence level of 'high' or 'very high' in at
390 least one of the ten analyses in this group and were considered to be in the virion.

391 Of the ten analyses performed with this method, 6 proteins were detected in only
392 one analysis. One of the proteins was found in 2 analyses, one in 3 analyses, 4 in four
393 analyses, 21 in 5 analyses, 2 in 6 analyses, 2 in 9 analyses, and 89 in all 10 analyses. The
394 number of analyses in which a protein is observed, can be influenced by either variability
395 inherent in mass spectrometry based proteomics experiments, variability in expression,
396 stability of the proteins or false positive results.

397 **Proteome is lower (L) strand and right hand side (R) biased.** The genes
398 predicted to encode proteins in the PBCV-1 genome are biased to the right side (262 of
399 416) relative to the mid-point of the genome; this is also reflected in the number of gene
400 products in the proteome (81 CDSs from right side, 67 CDSs from left side) (Fig. 3). In
401 addition, there is a bias to the reverse strand (L) for the right half of the genome in both
402 the total predicted proteins (159 of the 416, Fig. 3A) and the virion proteome (48 of 148,
403 Fig. 3B). This bias is consistent with certain viable PBCV-1 spontaneous large deletion
404 mutants where up to 40 kbp of the left side of the genome can be deleted (24, 54), and
405 these are recapitulated in the chlorovirus CVK2 (6). The right side L strand virion-
406 coding genes have a mean G+C content of 22%; whereas, the overall G+C content of the
407 genome is 40% and mean G+C content of all the coding genes is 31%. These
408 observations suggest the left side of the genome has less selection pressure relative to the
409 right side for the essential functions of virion assembly and maturation, The right side L

410 strand is relatively dense with virion-associated genes (38% of the total) with atypical
411 nucleotide composition; whereas, the corresponding left side of the genome is relatively
412 sparse (14%) with regards to virion proteins.

413 **Proteome is skewed to small basic proteins.** The PBCV-1 proteome has
414 proteins ranging in molecular weights from 4.9 to 143 kDa and in isoelectric points from
415 3.6 to 13.0, assuming no post-translational modifications (Fig. 4). Quantitatively, the
416 proteome is dominated by the MCP, centrally located in these distributions.
417 Qualitatively, the proteome is skewed to basic (~75%) and relatively small proteins,
418 approximately 50% are less than 20 kDa, and 63% of the proteins have molecular
419 weights less than 50 kDa and pI values greater than 7.0. This skewing to the more basic
420 side is interesting because the electrostatic charge of the 6×10^5 phosphate moieties in the
421 virus genome are probably neutralized by basic proteins (59). However, this prediction
422 must be evaluated further because the stoichiometry of the virion proteins is uncertain.
423 Additionally, how these relate to the chlorovirus CVK2 proteins with DNA binding and
424 protein kinase activities needs to be clarified (60).

425 Two-dimensional gel analyses using isoelectric focusing versus mass separations
426 support the skewing to basic and small proteins, suggesting that the majority of these
427 proteins are not post-translationally modified in such a way that causes significant
428 deviations of the predicted charge-mass migration (results not shown). However, we
429 never obtained good resolution of the proteins using 2-D gels, even though many
430 protocols were tried, because the MCP dominated the gel.

431 **Membrane proteins.** The virion proteins were evaluated for potential
432 transmembrane domains with three independent methods (20, 30, 50); these results

433 suggest that at least 26% of the proteome may be associated with a membrane structure
434 (Table 1), presumably the internal membrane of the virion. Two-thirds of the CDSs with
435 predicted transmembrane domains (3 out of 3 programs used) were detected by both
436 proteomic methods. The remaining 1/3 of the CDSs were detected equally with Method
437 1 biased to somewhat larger (mean MW = 23.8 kDa) and more basic proteins (mean pI =
438 9.2), whereas Method 2 was biased to smaller (mean MW = 10.3 kDa) and less basic
439 proteins (mean pI = 7.8).

440 The origin of the PBCV-1 internal membrane is unknown. If all, or at least most,
441 of the PBCV-1 internal membrane contains virus-encoded proteins and no host-encoded
442 proteins, it would suggest extensive modification of the host membrane to form the virus
443 membrane.

444 **PBCV-basic adaptor domain containing proteins.** Eight PBCV-1 CDSs have
445 at least one copy of a small, highly positively charged C-terminal domain, referred to as
446 the PBCV-basic adaptor domain (19): A092/093L, A176L, A205R, A278L, A282L,
447 A436L, A571R and A676R. All of these CDS were detected in the virion (Table 1).
448 These proteins range in size from 6.9 - 69 kDa, but their pI values are very basic, 10.6 -
449 13.0. Five of these proteins contain a single copy of the basic adaptor domain; however
450 A092/093L and A278L have 2 copies, and A282L has 3 copies. A278L and A282L are
451 S/T protein kinases (51). The A676R protein contains both the PBCV-basic adaptor
452 domain and a 2-cysteine domain (Pfam 08793), which is a virus-specific domain fused to
453 OUT/A20-like peptidases and S/T protein kinases and is suggested to function as a
454 targeting device for specific substrates (19). The PBCV-basic adaptor domain is only
455 found in the chloroviruses, and A176L is only found in PBCV-1. The function of the

456 PBCV-basic adaptor domain is unknown.

457 **MCP paralogs.** The initial understanding of the architectural makeup of the
458 PBCV-1 virion was a simple quasi-icosahedral particle consisting of a single MCP
459 (Vp54) (64). This picture has evolved to the present 8.5 Å resolution complex particle
460 with several surface features, including a unique vertex with a spike structure and fiber-
461 like structures associated with some capsomers in the trisymmetrons (5, 66). Genome
462 sequencing revealed genes encoding 6 additional capsid-like proteins (26). Previously
463 these paralogs were not considered relevant because at least two of them (genes *a010r*-
464 and *a011l*) could be deleted from the genome without loss of virion formation (24).
465 However, the proteome presented here indicates that all of the capsid-like proteins are
466 present in the virion (Table 1) and they fall into 5 paralog classes (Fig. 5A). Each of
467 these proteins contain 2 conserved domains [D1 (green) and D2 (red)] (Fig. 5B)
468 consistent with the Vp54 structure (Fig. 5C). The relative abundance of the proteins, as
469 estimated by their emPAI value, ranged from 1 (A384dL and A383R) to 13 (A430L and
470 A011L). These abundance ratios support the hypothesis that the architecture of-the
471 PBCV-1 virion is composed of a complex mixture of capsids and that the capsomers are
472 composed of heteromeric proteins with a conserved structure. Additionally, the 2 minor
473 capsid-like proteins, A383R and A384dL, contain an additional domain that is similar to
474 the chitin binding peritrophin-A domain (Pfam 01607.17) (SI Table S1) and may
475 contribute to the attachment of the virion to the algal cell surface. The relative abundance
476 of these proteins is consistent with the frequency of fiber structures found in each
477 trisymmetron, but the composition of these structures is unknown.

478 The estimated relative abundances of virion proteins were determined using the
479 emPAI method (18) for the Method 1 data set. The distribution of the capsid proteins
480 suggests a more complex assembly of PBCV-1 capsids than was previously assumed for
481 a single MCP (Vp54) responsible for the particle architecture. We assume the MCP
482 (A430L) is present in 1440 copies per virion for these calculations and other protein
483 abundances were estimated from this value (Fig. 5B). The data indicate there are two
484 capsid proteins of relatively high abundance (A430L and A011L), two capsid proteins
485 were present at approximately one-half the abundance of these (A010R and A558L), one
486 capsid protein present at one-third abundance (A622L), and two capsid proteins were
487 present in relatively low abundance (A383R and A384dL). Assuming these ratios,
488 icosahedral symmetry, and the fact that the virion is composed of 1680 capsids (64), each
489 of the triangular facets of the icosahedron would contain seven proteins in ratios of
490 72:72:36:36:24:1:1. Recent structural analysis of PBCV-1 at 8.5 Å resolution indicates
491 the capsomer volumes are more varied than previously thought (66), but how these
492 capsids are arranged is not known. The trimeric capsomers may be homomeric (as
493 previously thought), or possibly heteromeric utilizing the conserved beta-barrel domains
494 as binding surfaces. This higher complexity of virion structure is consistent with several
495 other large DNA viruses where multiple capsid proteins have been detected; herpes
496 viruses have 4 to 7 capsid proteins (22, 33) and mimivirus has at least 5 capsid proteins
497 (37). The emPAI method was used to estimate abundances of intracellular mature
498 virion proteins of vaccinia virus (7) indicating a dynamic range of 1 to 1000 with certain
499 core proteins being most abundant (i. e., A4L, A10L, F17R and A3L), as well as one with
500 low abundance (i. e., E11L).

501 **PBCV-1 proteome functionalities.** The 148 virion proteins were grouped into
502 11 functional/structural categories (SI Fig. S3A) and compared to the distribution of
503 CDSs of the overall genome (SI Fig. S3B). The majority (72%) of virion proteins are in
504 the unknown function category. However, several functions are inferred by sequence
505 similarity analyses and 13 of the 148 proteins have demonstrated functions that include
506 DNA binding, cell signaling via phosphorylation, DNA degradation, virus structure, cell
507 attachment, and polyamine biosynthesis such as homospermidine synthase. Among the
508 identified CDSs are the restriction endonucleases R.CviAII (A252R) and R.CviAI
509 (A579L) thought to be responsible for host DNA degradation early in the infection cycle
510 (3).

511 Virion morphogenesis is one of the last events in the PBCV-1 replication cycle
512 and it is reasonable that virion proteins are synthesized during the late phase. Most of the
513 proteome (87%) is from genes expressed either late or early-late (65); however, the time
514 of expression has not been determined for 23 new CDSs discovered with the resequence
515 and annotation (SI Fig. S2). Eleven proteins are from genes transcribed in the early
516 phase of replication: 7 of these proteins were detected by a single proteomic method with
517 a relatively low number of unique peptides detected. Therefore, these 7 proteins require
518 further verification. Three of these early proteins, A171R, A440L and A443R have
519 unknown functions. The A456L protein has two conserved domains, a D5 N superfamily
520 domain found in certain viral DNA primases (PfamA: PF08706.4) and a phage/plasmid
521 primase P4 family C-terminal domain with predicted ATPase activity. The A548L
522 protein has two conserved P-loop NTPase domains that are associated with DEXDc-,
523 DEAD- and DEAH-box proteins, including the hepatitis C virus NS3 helicases (PfamA:

524 PF00176.16). Thus, these proteins might contribute to early transcriptional events that
525 occur within minutes of infection.

526 **PBCV-1 packaged host protein.** The PBCV-1 proteome contains one protein
527 (101 amino acids) derived from the host (GenBank: EFN53917.1; 4); the protein was
528 detected by both proteomic methods. This protein is most similar to a fungal 93 amino
529 acid *Naumovozyma dairenensis* CBS 421 nucleosome binding protein (NCBI reference
530 sequence: XP_003667927.1) and similar to the HMGB-UBF_HMG-box, class II and III
531 members of the HMG-box superfamily of DNA-binding proteins. It has no similarity to
532 any PBCV-1 encoded protein. HMG-box containing proteins bind non-B-type DNA
533 conformations with high affinity (45) and they are involved in regulation of DNA-
534 dependent processes such as transcription, replication and DNA repair, all of which
535 require changing the conformation of chromatin (49). Thus, this host protein may be
536 important in initiating PBCV-1 gene expression, which occurs within minutes of
537 infection (65). At least two other large DNA viruses contain chromosomal proteins in the
538 virion. An HMG-box protein (HMG1) and a histone H2B.q protein occur in the Western
539 Reserve strain of vaccinia virus (38) and murine cytomegalovirus virions have a histone
540 H2A protein (22), suggesting large DNA viruses utilize host-derived proteins for DNA
541 binding functions.

542 **Presumed virion proteins that were not detected.** A few proteins were
543 expected to be packaged in PBCV-1 that were absent in the proteome analysis. As noted
544 previously, PBCV-1 packages one or more enzymes involved in digesting the host cell
545 wall during infection (29). Annotation of the PBCV-1 genome identified 5 enzymes that
546 might be involved in this process - two chitinases, a chitosanase, a β 1-3 glucanase and a

547 β & α 1,4 glucuronidase (SI Table S1). Recombinant proteins indicated that all of
548 these enzymes are functional (46, 47) and western blots suggested that one of the
549 chitinases and the chitosanase were in the virion (47). However, none of these five
550 proteins were detected in the proteome analysis. Consequently, the enzyme(s) involved
551 in digesting the host cell wall is unknown.

552 Circumstantial evidence suggests that PBCV-1 and other chloroviruses package a
553 small virus-encoded K^+ channel protein, named Kcv (12). It has been hypothesized that
554 Kcv is involved in depolarizing the host membrane, which occurs immediately after virus
555 infection. However, Kcv was not detected in this proteome study. On the other hand, at
556 least one putative protein (A201L) with predicted physical/chemical transmembrane
557 properties similar to Kcv was detected in the PBCV-1 virion with proteomic method 1.
558 Thus, this methodology can detect small proteins with transmembrane domains, as in
559 Kcv.

560 CONCLUSIONS

561 Re-sequencing and annotation of the 331 kbp chlorovirus PBCV-1 genome
562 revealed that the virus encodes 416 predicted CDSs, using a minimum ORF size of 40
563 codons, and 11 tRNAs. Proteome analysis of highly purified PBCV-1 virions identified
564 148 virus-encoded proteins (about 35% of the coding capacity of the virus) and one host
565 protein. Some of these proteins appear to be structural/architectural, whereas others have
566 enzymatic, chromatin modification and signal transduction functions. However, 106 of
567 these proteins have no known function or homologs in the existing gene databases except
568 as orthologs with other chloroviruses, phycodnaviruses and NCLDV. The genes
569 encoding these proteins are dispersed throughout the virus genome and 84% are

570 transcribed late or early-late in the infection cycle, which is consistent with virion
571 morphogenesis.

572 Probably the biggest surprise is that so many virus-encoded proteins were
573 detected in the virion and only one host encoded protein. However, except for the MCP
574 Vp54, we cannot definitively assign a protein(s) to any of the other structural features of
575 the virus, including the additional 6 major capsid-like proteins, the long spike structure,
576 the surface fibers on the trisymmetrons, or the long glue protein homologs of PRD1 and
577 the membrane protein dimer located at the edge of the trisymmetrons and internal
578 membrane (66). These await further structural analyses. Obviously one question is: Are
579 all of these virion-associated proteins essential for creating an infectious virus or are
580 some of them the result of 'sloppy packaging', i. e., fortuitously associated with the
581 particle. This is a difficult question to answer - but it is clear that PBCV-1
582 morphogenesis is selective in terms of what it incorporates; e.g., the virus packages 2
583 virus-encoded restriction endonucleases, but not their corresponding DNA
584 methyltransferases. In addition, only one host protein was detected in the virion; no host
585 membrane proteins were detected.

586 The PBCV-1 capsid protein composition may be somewhat flexible because the
587 genes encoding 2 of the capsid proteins (A010R and A011L) can be deleted (6, 24), yet
588 these deletion mutants are viable. This finding suggests some type of compensation in
589 capsid protein utility. Among large DNA viruses, the number of capsid proteins ranges
590 from 4 to 7 and these homologs are virion-associated (e. g., 22, 33, 37), thus the
591 discovery of 7 putative capsid proteins in the PBCV-1 virion is consistent with this theme
592 yet little is known how these proteins contribute to virion structure or function.

613

REFERENCES:

- 614 1. **Abrescia, N. G., J. J. Cockburn, J. M. Grimes, G. C. Sutton, J. M. Diprose, S.**
615 **J. Butcher, S. D. Fuller, C. San Martín, R. M. Burnett, D. I. Stuart, D. H.**
616 **Bamford, and J. K. Bamford.** 2004. Insights into assembly from structural
617 analysis of bacteriophage PRD1. *Nature* **432**:68-74.
- 618 2. **Agarkova, I., D. Dunigan, J. Gurnon, T. Greiner, J. Barres, G. Thiel, and J.**
619 **Van Etten.** 2008. Chlorovirus-mediated membrane depolarization of *Chlorella*
620 alters secondary active transport of solutes. *J. Virol.* **82**:12181-12190.
- 621 3. **Agarkova, I. V., D.D. Dunigan, J.L. Van Etten.** 2006. Virion-associated
622 restriction endonucleases of chloroviruses. *J. Virol.* **80**:8114-8123.
- 623 4. **Blanc, G., G. Duncan, I. Agarkova, M. Borodovsky, J. Gurnon, A. Kuo, E.**
624 **Lindquist, S. Lucas, J. Pangilinan, J. Polle, A. Salamov, A. Terry, T.**
625 **Yamada, D. Dunigan, I. Grigoriev, J.-M. Claverie, and J. L. Van Etten.** 2010.
626 The *Chlorella variabilis* NC64A genome reveals adaptation to photosymbiosis,
627 coevolution with viruses, and cryptic sex. *Plant Cell* **22**:2943-2955.
- 628 5. **Cherrier, M. V., V. A. Kostyuchenko, C. Xiao, V. D. Bowman, A. J. Battisti,**
629 **X. Yan, P. R. Chipman, T. S. Baker, J. L. Van Etten, and M. G. Rossmann.**
630 2009. An icosahedral algal virus has a complex unique vertex decorated by a
631 spike. *Proc Natl Acad Sci USA* **106**:11085-11089.
- 632 6. **Chuchird, N., K. Nishida, T. Kawasaki, M. Fujie, S. Usami, and T. Yamada.**
633 2002. A variable region on the chlorovirus CVK2 genome contains five copies of
634 the gene for Vp260, a viral-surface glycoprotein. *Virology* **295**:289-298.
- 635 7. **Chung, C.-S., C.-H. Chen, M.-Y. Ho, C.-Y. Huang, C.-L. Liao, and W.**

- 636 **Chang**, 2006. Vaccinia virus proteome: identification of proteins in vaccinia virus
637 intracellular mature virion particles. *J. Virol.* **80**:2127-2140.
- 638 8. **Cockburn, J., N. Abrescia, J. Grimes, G. Sutton, J. Diprose, J. Benevides, G.**
639 **J. Thomas, J. Bamford, D. Bamford, and D. Stuart.** 2004. Membrane structure
640 and interactions with protein and DNA in bacteriophage PRD1. *Nature* **432**:122-
641 125.
- 642 9. **Craig, R., and R. C. Beavis.** 2004. TANDEM: matching proteins with tandem
643 mass spectra. *Bioinformatics* **20**:1466-1467.
- 644 10. **Dereeper, A., V. Guignon, G. Blanc, S. Audic, S. Buffet, F. Chevenet, J. F.**
645 **Dufayard, S. Guindon, V. Lefort, M. Lescot, J. M. Claverie, and O. Gascuel.**
646 2008. Phylogeny.fr: robust phylogenetic analysis for the non-specialist. *Nucleic*
647 *Acids Res.* **36**:W465-469.
- 648 11. **Dunigan, D. D., L. A. Fitzgerald, and J. L. Van Etten.** 2006. Phycodnaviruses:
649 a peek at genetic diversity. *Virus Res.* **117**:119-132.
- 650 12. **Frohns, F., A. Käsmann, D. Kramer, B. Schäfer, M. Mehmel, M. Kang, J.L.**
651 **Van Etten, S. Gazzarrini, A. Moroni, G. Thiel.** 2006. Potassium ion channels of
652 chlorella viruses cause rapid depolarization of host cells during infection. *J. Virol.*
653 **80**:2437-2444.
- 654 13. **Graves, M. V., and R. H. Meints.** 1992. Characterization of the major capsid
655 protein and cloning of its gene from algal virus PBCV-1. *Virology* **188**:198-207.
- 656 14. **Higdon, R., G. Hather, A. T. Bauman, B. Louie, B. Broomall, S. Fortenly, N.**
657 **Kolker, G. van Belle, and E. Kolker.** 2009. SPIRE: systematic protein
658 identification and relative expression analysis resource for high-throughput

- 659 proteomics, 57th ASMS Conference on Mass Spectrometry, Philadelphia,
660 Pennsylvania, May 31 - June 4, 2009.
- 661 15. **Higdon, R., J. Hogan, N. Kolker, G. van Belle, and E. Kolker.** 2007.
662 Experiment-specific estimation of peptide identification probabilities using a
663 randomized database. *OMICS* **11**:351-356.
- 664 16. **Higdon, R., J. Hogan, G. Van Belle, and E. Kolker.** 2005. Randomized
665 sequence databases for tandem mass spectrometry peptide and protein
666 identification. *OMICS* **9**:364-379.
- 667 17. **Higdon, R., and E. Kolker.** 2007. A predictive model for identifying proteins by
668 a single peptide match. *Bioinformatics* **23**:277-280.
- 669 18. **Ishihama, Y., Y. Oda, T. Tabata, T. Sato, T. Nagasu, J. Rappsilber, and M.**
670 **Mann.** 2005. Exponentially modified protein abundance index (emPAI) for
671 estimation of absolute protein amount in proteomics by the number of sequenced
672 peptides per protein. *Mol. Cell Proteomics* **4**:1265-1272.
- 673 19. **Iyer, L., S. Balaji, E. Koonin, and L. Aravind.** 2006. Evolutionary genomics of
674 nucleo-cytoplasmic large DNA viruses. *Virus Res.* **117** 156-184.
- 675 20. **Käll, L., A. Krogh, and E. L. Sonnhammer.** 2004. A combined transmembrane
676 topology and signal peptide prediction method. *J. Mol. Biol.* **338**:1027-1036.
- 677 21. **Kang, M., D. D. Dunigan, and J. L. Van Etten.** 2005. Chloroviruses: a genus of
678 Phycodnaviridae that infect certain chlorella-like green algae. *Mol. Plant Path.*
679 **6**:213-224.
- 680 22. **Kattenhorn, L., R. Mills, M. Wagner, A. Lomsadze, V. Makeev, M.**
681 **Borodovsky, H. Ploegh, and B. Kessler.** 2004. Identification of proteins

- 682 associated with murine cytomegalovirus virions. *J. Virol.* **78**:11187-11197.
- 683 23. **Kuznetsov, Y. G., J. R. Gurnon, J. L. Van Etten, and A. McPherson.** 2005.
- 684 Atomic force microscopy investigation of a chlorella virus, PBCV-1. *J. Struct.*
- 685 *Biol.* **149**:256-263.
- 686 24. **Landstein, D., D. E. Burbank, J. W. Nietfeldt, and J. L. Van Etten.** 1995.
- 687 Large deletions in antigenic variants of the chlorella virus PBCV-1. *Virology*
- 688 **214**:413-420.
- 689 25. **Lane, L.** 1978. A simple method for stabilizing protein-sulfhydryl groups during
- 690 SDS-gel electrophoresis. *Anal. Biochem.* **86**:655-664.
- 691 26. **Li, Y., Z. Lu, L. Sun, S. Ropp, G. F. Kutish, D. L. Rock, and J. L. Van Etten.**
- 692 1997. Analysis of 74 kb of DNA located at the right end of the 330-kb chlorella
- 693 virus PBCV-1 genome. *Virology* **237**:360-377.
- 694 27. **Mehmel, M., M. Rothermel, T. Meckel, J.L. Van Etten, A. Moroni, G. Thiel.**
- 695 2003. Possible function for virus encoded K⁺ channel Kcv in the replication of
- 696 chlorella virus PBCV-1. *FEBS Lett.* **552**:7-11.
- 697 28. **Meints, R. H., D. E. Burbank, V. E. J.L., and L. D.T.** 1988. Properties of the
- 698 chlorella receptor for the virus PBCV-1. *Virology* **164**:15-21.
- 699 29. **Meints, R. H., K. Lee, D.E. Burbank, J.L. Van Etten.** 1984. Infection of a
- 700 chlorella-like alga with the virus, PBCV-1: Ultrastructural studies. *Virology*
- 701 **138**:341-346.
- 702 30. **Möller, S., M. D. R. Croning, and R. Apweiler.** 2001. Evaluation of methods
- 703 for the prediction of membrane spanning regions. *Bioinformatics* **17**:646-653.
- 704 31. **Nandhagopal, N., A. A. Simpson, J. R. Gurnon, X. Yan, T. S. Baker, M. V.**

- 705 **Graves, J. L. Van Etten, and M. G. Rossmann.** 2002. The structure and
706 evolution of the major capsid protein of a large, lipid-containing DNA virus. Proc
707 Natl Acad Sci USA **99**:14758-14763.
- 708 32. **Neupärtil, M., C. Meyer, I. Woll, F. Frohns, M. Kang, J.L. Van Etten, D.**
709 **Kramer, B. Hertel, A. Moroni, G. Thiel.** 2008. Chlorella viruses evoke a rapid
710 release of K⁺ from host cells during early phase of infection. Virology **372**:340-
711 348.
- 712 33. **O'Connor, C. M., and D. H. Kedes.** 2006. Mass spectrometric analyses of
713 purified rhesus monkey rhadinovirus reveal 33 virion-associated proteins. J. Virol.
714 **80**:1574-1583.
- 715 34. **Onimatsu, H., K. Suganuma, S. Uenoyama, and T. Yamada.** 2006. C-terminal
716 repetitive motifs in Vp130 present at the unique vertex of the chlorovirus capsid
717 are essential for binding to the host chlorella cell wall. Virology **353**:432-442.
- 718 35. **Onimatsu, H., I. Sugimoto, M. Fujie, S. Usami, and T. Yamada.** 2004. Vp130,
719 a chloroviral surface protein that interacts with the host Chlorella cell wall.
720 Virology **319**:71-80.
- 721 36. **Que, Q., Y. Li, I. N. Wang, L. C. Lane, W. G. Chaney, and J. L. Van Etten.**
722 1994. Protein glycosylation and myristylation in chlorella virus PBCV-1 and its
723 antigenic variants. Virology **203**:320-7.
- 724 37. **Renesto, P., C. Abergel, P. Decloquement, D. Moinier, S. Assa, H. Ogata, P.**
725 **Foruquet, J. P. Gorvel, and J. M. Claverie.** 2006. Mimivirus giant particles
726 incorporate a large fraction of anonymous and unique gene products. J. Virol.
727 **80**:11678-11685.

- 728 38. **Resch, W., K. K. Hixson, R. J. Moore, M. S. Lipton, and B. Moss.** 2007.
729 Protein composition of the vaccinia virus mature virion. *Virology* **358**:233-247.
- 730 39. **Santoni, V., M. Molloy, and T. Rabilloud.** 2000. Membrane proteins and
731 proteomics: Un amour impossible? *Electrophoresis* **21**:1054-1070.
- 732 40. **Shevchenko, A., M. Wilm, O. Vorm, and M. Mann.** 1996. Mass spectrometric
733 sequencing of proteins silver-stained polyacrylamide gels. *Anal. Chem.* **68**:850-
734 858.
- 735 41. **Short, C. M., O. Rusanova, and S. M. Short.** 2011. Quantification of virus
736 genes provides evidence for seed-bank populations of phycodnaviruses in Lake
737 Ontario, Canada. *ISME J.* **5**:810-821.
- 738 42. **Skrdla, M. P., D. E. Burbank, Y. Xia, R. H. Meints, and J. L. Van Etten.**
739 1984. Structural proteins and lipids in a virus, PBCV-1, which replicates in a
740 chlorella-like alga. *Virology* **135**:308-315.
- 741 43. **Song, W. J., Q. W. Qin, J. Qiu, C. H. Huang, F. Wang, and C. L. Hew.** 2004.
742 Functional genomics analysis of Singapore grouper iridovirus: complete sequence
743 determination and proteomic analysis. *J. Virol.* **78**:12576-12590.
- 744 44. **Stothard, P., and D. S. Wishart.** 2005. Circular genome visualization and
745 exploration using CGView. *Bioinformatics* **21**:537-539.
- 746 45. **Stros, M., D. Launholt, and K. D. Grasser.** 2007. The HMG-box: a versatile
747 protein domain occurring in a wide variety of DNA-binding proteins. *Cell. Mol.*
748 *Life Sci.* **64**:2590-2606.
- 749 46. **Sugimoto, I., H. Onimatsu, M. Fujie, S. Usami, and T. Yamada.** 2004. vAL-1,
750 a novel polysaccharide lyase encoded by chlorovirus CVK2. *FEBS Lett.* **559**:51-

- 751 56.
- 752 47. **Sun, L., B. Adams, J. Gurnon, Y. Ye, and J. L. Van Etten.** 1999.
- 753 Characterization of two chitinase genes and one chitosanase gene encoded by
- 754 chlorella virus PBCV-1. *Virology* **263**:376-387.
- 755 48. **Thiel, G., A. Moroni, D. Dunigan, and J. L. Van Etten.** 2010. Initial events
- 756 associated with virus PBCV-1 infection of *Chlorella* NC64A. *Prog. Bo.* **71**:169-
- 757 183.
- 758 49. **Thomas, J. O.** 2001. HMG1 and 2: architectural DNA-binding proteins.
- 759 *Biochem. Soc. Trans.* **29**:395-401.
- 760 50. **Tusnády, G. E., and I. Simon.** 2001. The HMMTOP transmembrane topology
- 761 prediction server. *Bioinformatics* **17**:849-850.
- 762 51. **Valbuzzi, P.** 2005. Serine/threonine kinases encoded by PBCV-1 virus:
- 763 characterization and possible role in the phosphorylation of the K⁺ channel Kev.
- 764 Ph. D. Dissertation. Universita Degli Studi di Milano, Italy.
- 765 52. **Van Etten, J. L., D. E. Burbank, D. Kuczmarski, and R. H. Meints.** 1983.
- 766 Virus infection of culturable chlorella-like algae and development of a plaque
- 767 assay. *Science* **219**:994-996.
- 768 53. **Van Etten, J. L., D.E. Burbank, Y. Xia, R.H. Meints.** 1983. Growth cycle of a
- 769 virus, PBCV- 1, that infects chlorella-like algae. *Virology* **126**:117-125.
- 770 54. **Van Etten, J. L., and D. D. Dunigan.** 2012. Chloroviruses: not your every day
- 771 plant virus. *Trends Plant Sci.* **17**:1-8.
- 772 55. **Van Etten, J. L., M. V. Graves, D. G. Muller, W. Boland, and N. Delaroque.**
- 773 2002. Phycodnaviridae-large DNA algal viruses. *Arch. Virol.* **147**:1479-1516.

- 774 56. **Van Etten, J. L., L. C. Lane, and R. H. Meints.** 1991. Viruses and viruslike
775 particles of eukaryotic algae. *Microbiol. Rev.* **55**:586-620.
- 776 57. **Van Etten, J. L., and R. H. Meints.** 1999. Giant viruses infecting algae. *Annu.*
777 *Rev. Microbiol.* **53**:447-494.
- 778 58. **Van Etten, J. L., C. H. Van Etten, J. K. Johnson, and D. E. Burbank.** 1985. A
779 survey for viruses from fresh water that infect a eucaryotic chlorella-like green
780 alga. *Appl. Environ. Microbiol.* **49**:1326-1328.
- 781 59. **Wulfmeyer, T., C. Polzer, G. Hiepler, K. Hamacher, R. Shoeman, D. D.**
782 **Dunigan, J. L. Van Etten, M. Lolicato, A. Moroni, G. Thiel, and T. Meckel.**
783 2012. Structural organization of DNA in chlorella viruses. *PLoS One* **7**:e30133.
- 784 60. **Yamada, T., S. Furukawa, T. Hamazaki, and P. Songsri.** 1996.
785 Characterization of DNA-binding proteins and protein kinase activities in
786 chlorella virus CVK2. *Virology* **219**:395-406.
- 787 61. **Yamada, T., T. Higashiyama, and T. Fukuda.** 1991. Screening of natural
788 waters for viruses which infect chlorella cells. *Appl. Environ. Microbiol.*
789 **57**:3433-3437.
- 790 62. **Yamada, T., H. Onimatsu, and J. L. Van Etten.** 2006. Chlorella viruses, p.
791 293-366. *In* K. Maramorosch and A. J. Shatkin (ed.), *Adv. Virus Res.*, vol. 66.
792 Elsevier Inc.
- 793 63. **Yan, X., V. Bowman, N. H. Olson, J. R. Gurnon, J. L. Van Etten, M. G.**
794 **Rossmann, and T. S. Baker.** 2005. The structure of a T=169d algal virus,
795 PBCV-1, at 15 Å resolution. *Microsc. Microanal.* **11**:1056-1057.
- 796 64. **Yan, X., N. H. Olson, J. L. Van Etten, M. Bergoin, M. G. Rossmann, and T.**

- 797 **S. Baker.** 2000. Structure and assembly of large lipid-containing dsDNA viruses.
798 Nat. Struct. Biol. **7**:101-103.
- 799 65. **Yanai-Balsler, G. M., G. A. Duncan, J. D. Eudy, D. Wang, X. Li, I. V.**
800 **Agarkova, D. D. Dunigan, and J. L. Van Etten.** 2010. Microarray analysis of
801 chlorella virus PBCV-1 transcription. J.Virol. **84**:532-542.
- 802 66. **Zhang, X., Y. Xiang, D. D. Dunigan, T. Klose, P. R. Chipman, J. L. Van**
803 **Etten, and M. G. Rossmann.** 2011. Three-dimensional structure and function of
804 the *Paramecium bursaria* chlorella virus capsid. Proc Natl Acad Sci USA
805 **108**:14837-14842.
- 806 67. **Zhang, Y., I. Calin-Jageman, J. R. Gurnon, T. J. Choi, B. Adams, A. W.**
807 **Nicholson, and J. L. Van Etten.** 2003. Characterization of a chlorella virus
808 PBCV-1 encoded ribonuclease III. Virology **317**:73-83.
- 809 68. **Zhang, Y., P. Strasser, R. Grabherr, and J. L. Van Etten.** 1994. Hairpin loop
810 structure at the termini of the chlorella virus PBCV-1 genome. Virology
811 **202**:1079-1082.

812

Figure legends

813 **Figure 1.** Proteomic methodologies for PBCV-1 virions.

814 **Figure 2.** SDS-PAGE protein separation and virion proteome mapped onto the PBCV-1
815 genome. The PBCV-1 genome was re-sequenced, assembled and annotated to correct
816 existing sequence errors. The 416 predicted CDSs are represented as grey arrows
817 running both clockwise and counter-clockwise along the genome (panel B). Note: the
818 diagram is circular, but there is a break at the 12 o'clock position because the viral
819 genome is a linear molecule with terminal inverted repeats and closed hairpin ends. The
820 terminal sequences (inverted repeats and hairpin ends) were found to be identical to those
821 reported previously (68). The polycistronic gene encoding 11 tRNAs is presented in red
822 (see 6 o'clock). The 148 proteins of the virion proteome were determined using two
823 independent mass spectrometry-based methods (see Materials and Methods). The results
824 of each method are shown, proteins determined uniquely by method 1 are presented in
825 magenta, proteins determined uniquely by method 2 are presented in blue, proteins
826 determined by both methods 1 and 2 are presented in brown. The map was developed
827 from the CGView software (44). Panel A shows the distribution of virion proteins with
828 SDS polyacrylamide gel separation. The numbers to the left indicate the gel fragment
829 that was analyzed.

830 **Figure 3.** Expression stage distribution of PBCV-1 CDSs, a quartile analysis. The
831 number of all coding CDSs (panel A) expressed either during the early (blue), early-late
832 (red), late (green), or not determined (nd, purple) is shown as a function of the genome
833 map position. The genome map is divided into four regions, both the direct ("R" genes)

834 and reverse (“L” genes) on each half of the genome (left half gene numbers: 001 – 327;
835 right half gene numbers: 328 – 692). Panel B shows the distribution of virion-associated
836 CDSs with respect to expression stage and genome position.

837 **Figure 4.** Mass versus pI distribution of PBCV-1 virion CDSs identified by two
838 independent proteomic methods. The virion proteins are displayed as a function of their
839 intrinsic molecular weight and isoelectric point. The results of each method are shown,
840 proteins determined uniquely using method 1 are presented in magenta, proteins
841 determined uniquely using method 2 are presented in blue, proteins determined using
842 both methods 1 and 2 are presented in brown. Note that Method 2 was especially useful
843 for discovering a set of low molecular weight proteins that were not detected with
844 Method 1.

845 **Figure 5.** Capsid protein paralog classes and relative abundances in PBCV-1. The seven
846 capsid-like proteins detected in the PBCV-1 virion were evaluated against a dataset of
847 chloroviruses, including PBCV-1 (RefSeq NC_000852.5), NY-2A (RefSeq
848 NC_009898.1), AR158 (RefSeq NC_009899.1), MT325 (GenBank DQ491001.1), FR483
849 (RefSeq NC_008603.1), and ATCV-1 (RefSeq NC_008724.1). These 7 proteins had
850 homologs in each of the viruses that separate into 5 distinct paralog classes (I – V) as
851 shown in the neighbor joining tree (panel A) (see SI Table S3 for CDS accession
852 numbers). The sequence for PBCV-1 A384dL, a member of paralog class V which is
853 distantly related, was used as the out-group to root the phylogenetic analysis using the
854 website www.phylogeny.fr (10). Muscle was used to align the sequences. Bootstrap
855 analysis was used to construct the tree. Similar tree topologies were produced by

856 maximum likelihood and maximum parsimony analyses. The values on the branches are
857 the percentage of bootstrap support (200 replicates). Only bootstrap values >50% are
858 shown. The distance bar represents 0.2 amino acid substitution per site. Panel B presents
859 the PBCV-1 capsid proteins grouped into 5 paralog classes within their two conserved
860 domains. The D1 domain (green, column A) and the D2 (red, column D) NCLDV
861 superfamily capsid domain were previously determined by structure analysis of the Vp54
862 MCP (31) (panel C). The relative abundances as determined with the emPAI method for
863 the Method 1 data are listed to the right of the table, as well as the hypothetical estimated
864 copies per virion of each capsid protein. Note, the two proteins of relatively lower
865 abundance contain chitin binding peritrophin-A conserved domains (columns C and E).

866 Table 1. PBCV-1 virion proteome

Protein (CDS)	Da	pI	Expression stage	Function or putative function	Proteomic method	TM prediction ^a		
						T	H	P
A010R	44998	5.2	Late	Capsid protein; PfamA: PF4451.5 [1.9e-50]	1&2	0	0	0
A011L	45076	5.4	Late	Capsid protein; PfamA: PF4451.5 [2.9e-61]	1&2	0	0	0
A014R	141382	6.3	Late	Unknown protein	1&2	0	0	0
A018L	137639	4.9	Late	Unknown protein; PfamA: PF06598.4 [Chlorovirus glycoprotein repeat] [1.2e-11]	1	0	0	0
A025/027/029L	140095	4.4	Late	Unknown protein	1&2	0	0	0
A034R	35163	10.4	Late	Protein kinase; PfamA: PF00069.18 [Protein kinase domain] [1.4e-07]	1&2	0	1	0
A035L	65606	8.9	Late	Unknown protein	1&2	0	1	0
A041R	44315	10.8	Late	Unknown protein	1&2	0	1	0
A051L	22804	8.6	Late	Unknown protein	1&2	1	2	1
A085R	27812	7.8	Late	Prolyl 4-hydroxylase; PfamA: PF03171.13 [2OG-Fe(II) oxygenase superfamily] [3.5e-11]	1&2	1	1	1
A092/093L	49577	10.7	Early-Late	Unknown protein; PfamA: PF08789.3 [PBCV-specific basic adaptor domain] [1.2e-15]	1&2	0	0	0
A121R	12486	10.8	Early-Late	Unknown protein	1&2	0	0	0
A122/123cL	4912	10.1	N/A	Unknown protein	1	0	0	0
A122/123R	137880	5.0	Late	COG5295 [Autotransporter adhesin] [4e-12]; PfamA: PF06598.4 [Chlorovirus glycoprotein repeat] [3.6e-11] / PF11962.1 [Domain of unknown function (DUF3476)] [8.2e-66]	1	0	31	0
A127R	27126	10.1	Late	Unknown protein	1&2	0	0	0
A136R	16367	11.5	N/A	Unknown protein	1&2	0	0	0
A137R	8777	10.9	Early	Unknown protein	1	0	0	0

A139L	17701	8.4	Late	Unknown protein	1&2	2	2	2
A140/145R	120898	11.0	Early-Late	Unknown protein	1&2	0	1	0
A157L	12328	3.9	Early-Late	Unknown protein	2	1	1	1
A164aR	7094	5.8	N/A	Unknown protein	2	1	0	0
A165aL	19024	10.1	N/A	Unknown protein	1&2	0	0	0
A168R	18317	4.6	Late	Unknown protein	1&2	1	1	1
A171R	42413	10.2	Early	Unknown protein	1&2	0	0	0
A172aL	6053	9.8	N/A	Unknown protein	1	1	1	0
A173L	31933	8.2	Early	COG1752 [Predicted esterase of the alpha-beta hydrolase superfamily] [2e-06]; PfamA: PF01734.15 [Patatin-like phospholipase] [4.2e-27]	1	0	2	0
A174L	7453	12.2	N/A	Unknown protein	2	0	0	0
A176L	9167	11.3	N/A	Unknown protein; PfamA: PF08789.3 [PBCV-specific basic adaptor domain] [9e-12]	1&2	0	0	0
A188aR	17326	10.0	N/A	COG0417 [DNA polymerase elongation subunit (family B)] [3e-07]; PfamA: PF00136.14 [DNA polymerase family B] [6.5e-17]	1	0	0	0
A189/192R	143575	11.4	Late	Unknown protein	1&2	0	0	0
A196L	17456	8.4	Late	Unknown protein	2	3	3	1
A201aL	6787	8.8	N/A	Unknown protein	1	0	0	0
A201L	10005	10.7	Early-Late	Unknown protein	1	2	2	2
A202L	12232	5.0	Early-Late	Unknown protein	2	0	0	0
A203R	24011	6.0	Late	Unknown protein	1&2	1	2	0
A205R	22452	12.1	Late	Unknown protein; PfamA: PF08789.3 [PBCV-specific basic adaptor domain] [4.2e-16]	1&2	0	0	0
A213L	16483	4.5	Early-Late	Unknown protein	1&2	1	1	1
A217L	45248	9.9	Early-Late	Unknown protein	1&2	0	0	1
A219/222/226R	77797	7.0	Early	COG1215 [Glycosyltransferases probably involved in cell wall biogenesis] [4e-06]; Swissprot: P58932 [RecName: FullCellulose synthase catalytic subunit (UDP-forming)]	1	9	8	10

[6e-07]

A227L	15689	10.0	Late	Unknown protein	1&2	0	0	0
A230R	22055	8.4	Late	Unknown protein	1&2	4	4	4
A231L	43644	9.9	Early-Late	Unknown protein	1&2	1	0	0
A237R	58565	9.5	Late	Homospermidine synthase	1&2	0	0	0
A245R	19748	9.3	Late	Cu/Zn superoxide dismutase	1&2	1	1	0
A246R	12017	11.5	Late	Unknown protein	1&2	0	0	0
A252R	39856	10.3	Early	R.CviAII restriction endonuclease	1&2	0	0	0
A255R	17300	5.1	N/A	Unknown protein	1	0	0	0
A256/257L	96729	7.2	Early-Late	Unknown protein	1	0	0	0
A260aR	7742	11.9	N/A	Unknown protein	1	0	0	0
A262/263L	29470	9.6	N/A	Unknown protein	1&2	2	3	2
A271L	31114	7.1	Early-Late	COG2267 [Lysophospholipase] [1e-07]	1	0	3	0
A273L	15713	9.9	Late	PF03713.6 [Domain of unknown function (DUF305)] [6.8e-13]	1	3	3	3
A278L	69231	10.8	Late	Protein kinase; PfamA: PF00069.18 [Protein kinase domain] [1.2e-07] / PF08789.3 [PBCV-specific basic adaptor domain] [7.5e-10]	1&2	0	1	0
A282L	63371	10.8	Late	Protein kinase; PfamA: PF00069.18 [Protein kinase domain] [1.2e-07] / PF08789.3 [PBCV-specific basic adaptor domain] [1.3e-17]	1&2	0	1	0
A284L	30766	9.2	Early-Late	Amidase	1&2	0	0	0
A286R	43042	9.6	Late	Unknown protein	1&2	0	0	0
A287R	31349	9.4	Early-Late	PfamA: PF01541.17 [GIY-YIG catalytic domain] [4.2e-11] / PF07453.6 [NUMOD1 domain] [8.6e-11]	1	0	0	0
A295L	35626	7.9	Early-Late	Fucose synthetase; Swissprot: Q9LMU0 [RecName: FullPutative GDP-L-fucose synthase 2 AltName: FullGDP-4-keto-6-deoxy-D-mannose-3 5-epimerase-4-reductase 2 ShortAtGER2] [1e-100]	1	0	0	0

A296R	17393	12.2	Late	Unknown protein	1&2	0	1	1
A304R	9490	5.8	Late	Unknown protein	1	0	0	0
A305L	22910	10.7	Late	Protein phosphatase; Swissprot: Q9BY84 [RecName: FullDual specificity protein phosphatase 16 AltName: FullMitogen-activated protein kinase phosphatase 7 ShortMAP kinase phosphatase 7 ShortMKP-7] [7e-12]	1&2	0	0	0
A310L	18268	8.5	Late	Unknown protein	1&2	0	0	0
A314R	9114	6.7	Late	Unknown protein	1&2	1	1	1
A316R	48779	10.7	Late	Unknown protein	1&2	0	1	0
A320R	15685	10.5	Late	Unknown protein	1&2	1	1	1
A321R	12830	8.8	Late	Unknown protein	1	2	2	2
A322L	20039	5.0	Late	Unknown protein	1&2	1	1	1
A339L	7372	11.1	Early-Late	Unknown protein	1	0	0	0
A342L	63813	9.2	Early-Late	Unknown protein	1&2	1	1	1
A349L	21077	10.0	Early-Late	Unknown protein	1&2	0	1	0
A350R	14676	9.7	N/A	PfamA: PF12239.1 [Protein of unknown function (DUF3605)] [4.4e-23]	2	0	0	0
A352L	23310	3.6	Late	Swissprot: Q5UQF7 [RecName: FullUncharacterized protein R489 Flags: Precursor] [1e-05]	1&2	0	1	1
A356R	12512	10.5	N/A	Unknown protein	1	0	0	0
A363R	128448	10.9	Early	Swissprot: P0C9B2 [RecName: FullPutative ATP-dependent RNA helicase Q706L] [2e-06]	1&2	0	2	0
A375R	19085	9.4	Early-Late	Unknown protein	1&2	2	2	2
A378L	29219	9.4	Late	Unknown protein	1&2	1	1	0
A383R	52511	5.2	Late	Capsid protein; Pfam: PF04451.5 [Large eukaryotic DNA virus major capsid protein] [1.6e-25]	1&2	0	0	0
A384bL	6809	9.0	N/A	Unknown protein	2	1	1	1
A384dL	69009	8.0	Early-Late	Capsid protein; PfamA: PF01607.17 [Chitin binding Peritrophin-A domain] [2.4e-07] / PF04451.5 [Large eukaryotic DNA virus	1&2	1	2	1

major capsid protein] [2e-11]

A398L	12987	9.9	Late	Unknown protein	1&2	2	3	3
A400R	13634	9.5	Early-Late	Unknown protein	2	0	0	0
A405R	53502	10.3	Late	Unknown protein	1&2	1	2	1
A407L	23382	8.9	Late	Unknown protein	1&2	1	2	2
A413L	26998	9.5	Late	Unknown protein	1&2	2	2	2
A414R	10612	10.8	Late	Unknown protein	1&2	2	2	2
A420L	7918	6.4	Late	Unknown protein	2	1	1	1
A421R	11056	10.1	Late	Unknown protein	1&2	1	1	1
A423R	18458	6.5	Late	Unknown protein	2	0	1	0
A430L	48165	7.5	Late	Major capsid protein	1&2	0	0	0
A436L	6932	13.0	N/A	Unknown protein; Pfam: PF08789.3 [PBCV-specific basic adaptor domain] [1.5e-16]	1	0	0	0
A437L	10876	11.0	Late	PfamA: PF05854.4 [Non-histone chromosomal protein MC1] [5.9e-07]	1&2	0	1	0
A438L	8988	10.7	Early-Late	Glutaredoxin	2	0	0	0
A440L	10112	11.1	Early	Unknown protein	1&2	0	0	0
A443R	34961	5.3	Early	Unknown protein	1	0	0	0
A448L	12369	10.4	Late	Protein disulphide isomerase with heme binding site	1&2	0	0	0
A454L	31194	4.7	Early-Late	Unknown protein	1&2	1	1	0
A456L	75235	5.5	Early	COG3378 [Predicted ATPase] [3e-06]; PfamA: PF08706.4 [D5 N terminal like] [3.9e-09]	1	0	0	0
A465R	13528	10.2	Early-Late	COG5054 [Mitochondrial sulfhydryl oxidase involved in the biogenesis of cytosolic Fe/S proteins] [4e-06]; PfamA: PF04777.6 [Erv1 / Alr family] [3.5e-22]	1&2	0	0	0
A476R	37393	4.4	Early-Late	Swissprot: Q6Y657 [RecName: FullPutative ribonucleoside-diphosphate reductase small chain B AltName: FullRibonucleotide reductase small subunit B AltName: FullRibonucleoside-diphosphate reductase	1	0	0	1

R2B subunit] [1e-113]

A480L	9838	10.0	Late	Unknown protein	1&2	2	2	2
A484L	18604	9.6	Early-Late	Unknown protein	1&2	0	0	0
A488R	34631	5.0	Late	Swissprot: Q5UQL4 [RecName: FullUncharacterized protein L417] [2e-09]	1&2	0	3	0
A497R	15378	10.4	Late	Unknown protein	1&2	2	2	1
A500L	38463	5.0	N/A	Unknown protein	1&2	1	2	1
A502L	11069	9.4	Late	Unknown protein	2	1	1	1
A520L	11674	10.7	Late	Unknown protein	2	0	0	0
A521aL	22578	6.3	N/A	Swissprot: O55742 [RecName: FullUncharacterized protein 136R] [2e-07]	1&2	0	0	0
A521L	23738	11.4	Early-Late	Unknown protein	1&2	0	0	0
A523R	19096	9.6	Late	Unknown protein	1&2	0	0	0
A526R	16434	9.3	Late	Unknown protein	1&2	0	1	0
A527R	11605	10.7	Late	Unknown protein	1&2	0	0	0
A531L	7670	7.5	Late	Unknown protein	2	1	1	1
A532aL	5479	4.5	N/A	Unknown protein	2	1	1	1
A532L	8698	9.7	Late	Unknown protein	1&2	1	1	1
A533R	40132	3.8	Early-Late	Unknown protein	1&2	0	0	0
A534R	11783	9.7	N/A	Unknown protein	1&2	0	0	0
A535L	8210	4.7	Early-Late	Unknown protein	1&2	0	0	0
A536L	8485	10.0	Early-Late	Unknown protein	1&2	1	1	0
A540L	127197	6.2	Late	Unknown protein	1	0	0	0
A548L	57432	9.5	Early	PfamA: PF00176.16 [SNF2 family N-terminal domain] [6.7e-34] / PF00271.24 [Helicase conserved C-terminal domain] [1.5e-10]	1	0	0	0
A558L	45547	5.1	Early-Late	Capsid protein; PfamA: PF04451.5 [Large eukaryotic DNA virus major capsid protein] [6.6e-60]	1&2	0	0	0
A559L	24034	10.2	Late	Unknown protein	1&2	1	1	0

A561L	71004	9.9	Late	Unknown protein	1&2	1	2	1
A565R	73169	7.3	Early-Late	Unknown protein	1&2	1	1	1
A567L	17418	10.1	Early-Late	Unknown protein	1	0	0	0
A571R	12972	12.0	Late	Pfam hit: PF08789.3 [PBCV-specific basic adaptor domain] [5.7e-17]; Refseq best hit: YP_001426112 [hypothetical protein FR483_N480R (Paramecium bursaria Chlorella virus FR483)] [3e-39]	1	0	0	0
A572R	20606	7.1	Late	Unknown protein	1&2	0	0	0
A577L	15442	11.0	Late	Unknown protein	1&2	0	0	0
A579L	27445	10.1	Late	R.CviAI restriction endonuclease	1&2	0	0	0
A586R	8567	11.8	N/A	Unknown protein	1	0	0	0
A598L	41558	6.9	Early-Late	COG0076 [Glutamate decarboxylase and related PLP-dependent proteins] [5e-06]; PfamA: PF00282.12 [Pyridoxal-dependent decarboxylase conserved domain] [1.1e-17]	1	0	0	0
A605L	17769	10.9	Early-Late	Unknown protein	1&2	1	1	1
A612L	13587	8.7	Late	Histone H3K27 methylase	2	0	0	0
A614L	64733	11.2	Late	Protein kinase; PfamA: PF00069.18 [Protein kinase domain] [5.6e-11]	1&2	0	0	0
A617R	37586	9.9	Early-Late	Swissprot: Q5UQJ6 [RecName: FullPutative serine/threonine-protein kinase R400] [7e-12]	1	0	0	0
A621L	12935	9.5	Late	Unknown protein	1	2	2	2
A622L	58097	5.7	Late	Capsid protein; PfamA: PF04451.5 [Large eukaryotic DNA virus major capsid protein] [1.7e-66]	1&2	0	0	0
A624R	13570	9.3	Late	Unknown protein; PfamA: PF09945.2 [Predicted membrane protein (DUF2177)] [3.4e-26]	1	3	4	3
A625R	49945	10.7	Late	COG0675 [Transposase and inactivated derivatives] [1e-06]; PfamA: PF12323.1 [Helix-turn-helix domain] [1.4e-06] / PF07282.4 [Putative transposase DNA-binding domain] [6.7e-18]	1	0	0	0
A627R	49629	11.1	Late	Unknown protein	1&2	1	3	0

Page 47 of 47

A629R	86292	7.5	Early-Late	PfamA: PF03477.9 [ATP cone domain] [8.5e-15] / PF00317.14 [Ribonucleotide reductase all-alpha domain] [7.9e-19] / PF02867.8 [Ribonucleotide reductase barrel domain] [2e-194]	1	0	0	0
A631L	10392	9.9	N/A	Unknown protein	1	0	0	0
A643R	53097	11.3	Late	Unknown protein	1&2	0	0	0
A644R	19207	6.0	Late	Unknown protein	1&2	0	0	0
A655L	12002	11.4	N/A	Unknown protein	1	0	1	0
A676R	42432	10.6	Late	Unknown protein; PfamA: PF08789.3 [PBCV-specific basic adaptor domain] [1.9e-17] / PF08793.3 [2-cysteine adaptor domain] [1.8e-15]	1&2	0	0	0
A678R	41287	10.3	Late	Unknown protein	1&2	0	3	0
A686L	18316	6.9	Early	Unknown protein	1	0	1	0

867 a – Transmembrane regions of the protein were predicted by TMHMM [T] (30), HMMTOP [H] (50), and Phobius [P] (20) methods.

868 For all the method default parameters were used for the prediction. The number shown in the table is the number of helices predicted

869 by the method.

Virus purification:
 Differential centrifugation
 Protease-wash
 Rate-zonal gradient centrifugation Isopycnic
 gradient centrifugation

Method 1
SDS-PAGE/Trypsin/HPLC/Ion Spray/ MS-MS

Virus solubilization:
 +/- alkylation
 Reduction
 +/- phenol or phenol-toluene extraction
 SDS/crystal violet/Ficoll
 100 °C

Protein separation and fragmentation:
 One-dimensional SDS-PAGE
 Sypro-Ruby staining
 Gel slices
 Imbibe with trypsin
 Eluted tryptic fragments

Peptide separation:
 Tryptic fragments injected onto C-18
 reverse phase LC

Mass spectrometry:
 Electrospray ionization injection
 Q-TOF Ultima
 MS/MS acquisitions – 60 to 1900 daltons

Mass ion analyses:
 Masslynx produce peak lists
 MASCOT to NCBI (nr database)
 Mass accuracy at 0.1 daltons
 Protein identification: $p < 0.5$

Relative abundance:
 emPAI

Method 2
PPS/Trypsin/HPLC/MS-MS

Virus solubilization:
 PPS
 100 °C
 Reduction
 Alkylation

Protein fragmentation:
 Trypsin
 Acid to hydrolyse PPS

Peptide separation:
 Tryptic fragments injected onto C-18
 reverse phase LC

Mass spectrometry:
 LTQ-Velos or LCQ Deca XP Plus
 MS/MS acquisitions – exclusion list 100
 daltons

Mass ion analyses:
 Xcalibur produced peak lists
 X!Tandem and SPIRE to custom
 DB
 Mass Accuracy at 2.5 Da
 Protein identification $\leq 1\%$ FDR

Figure 1

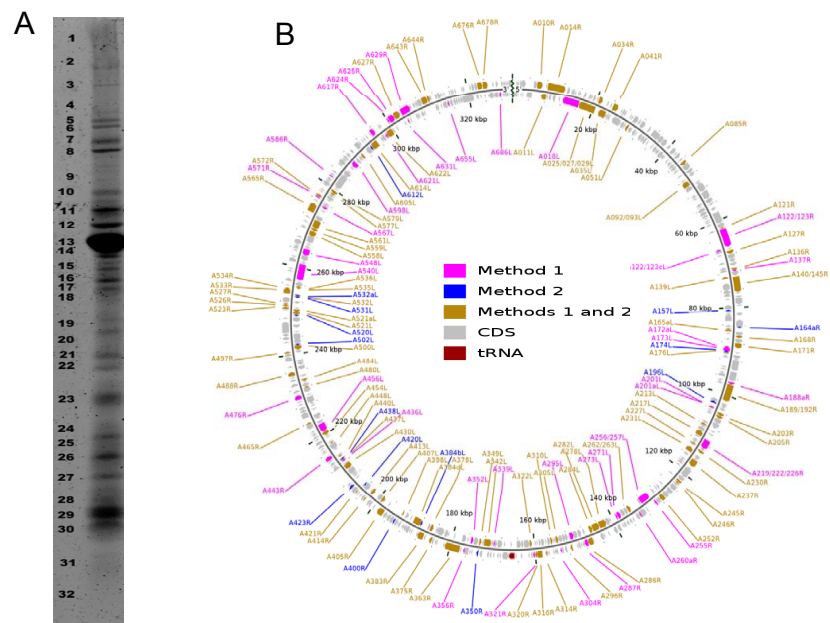


Figure 2.

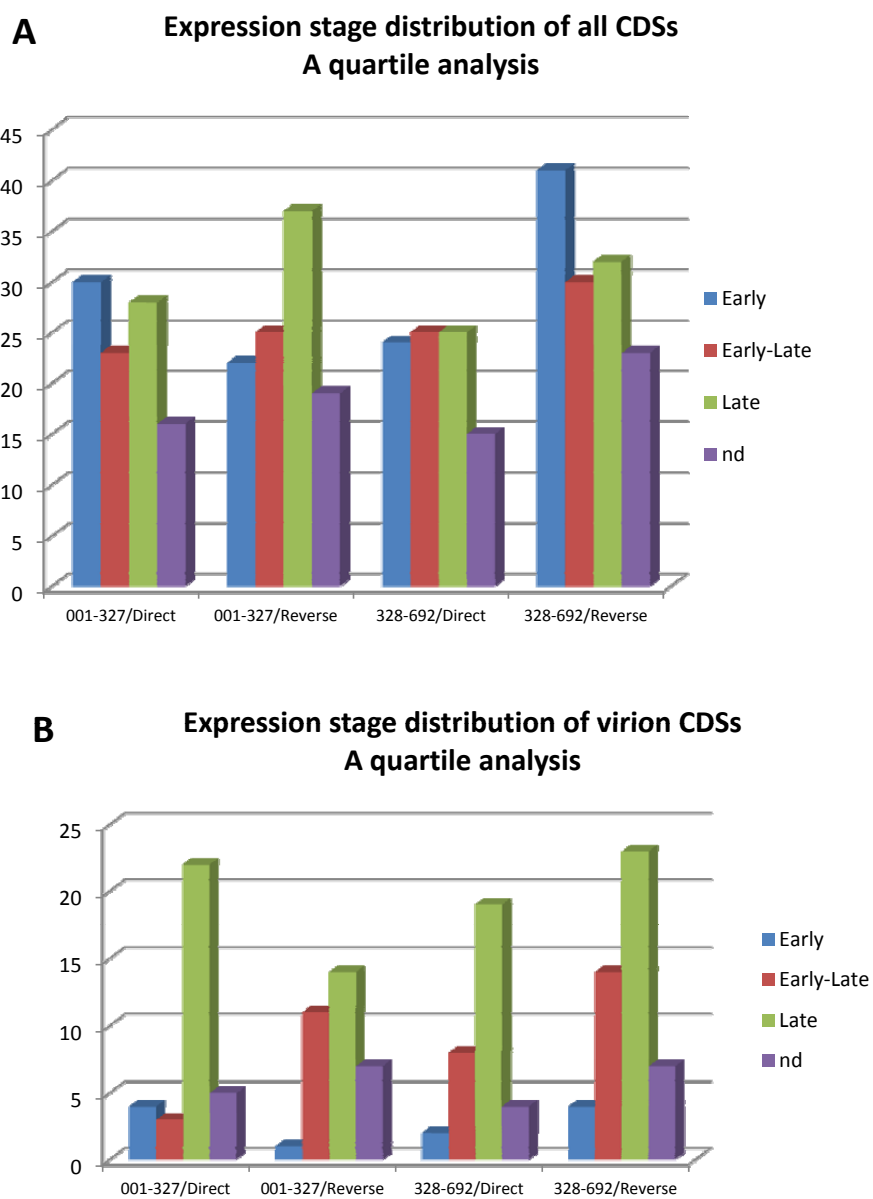


Figure 3

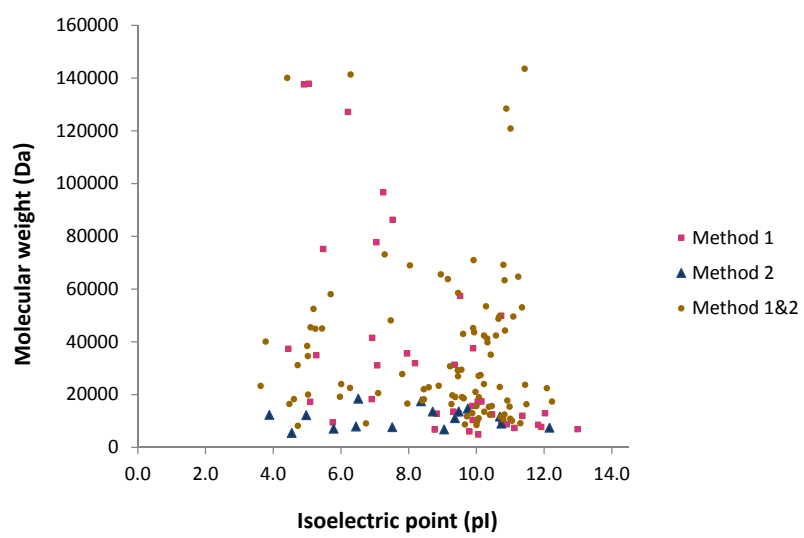


Figure 4

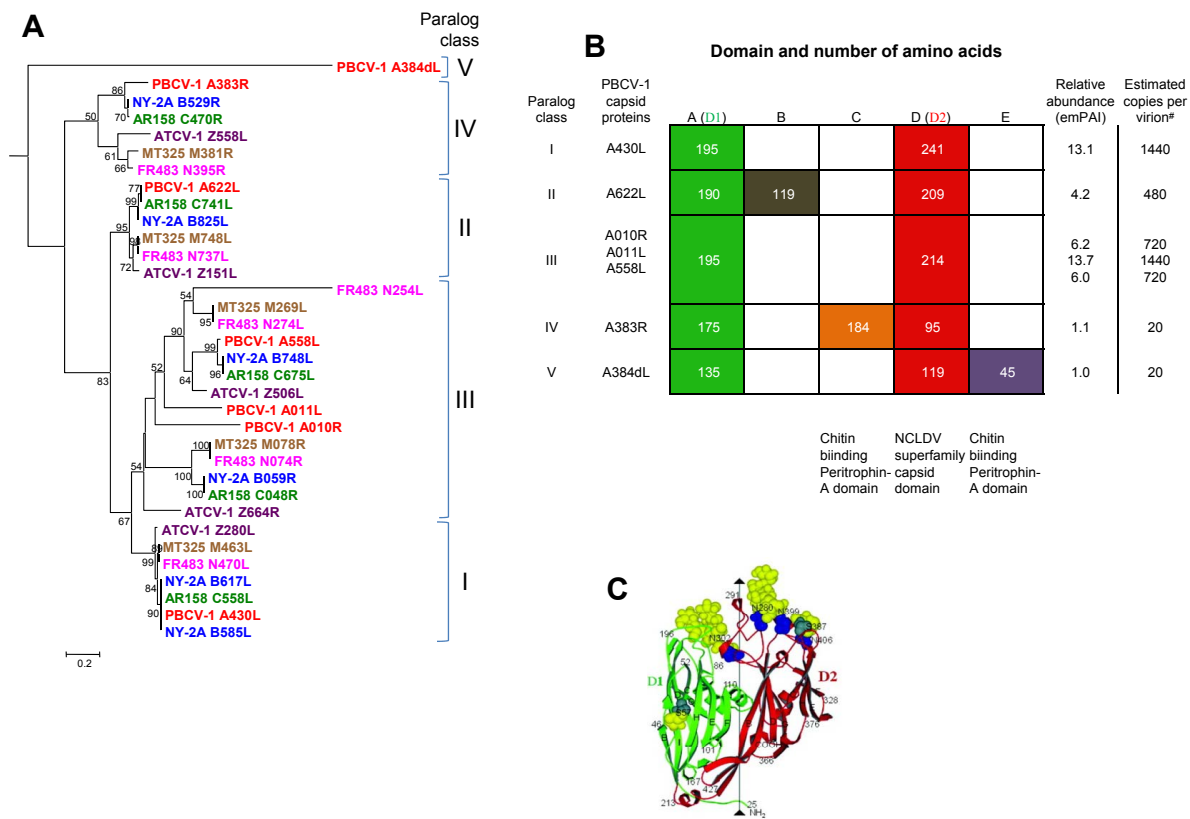


Fig. 5